

# Marine natural products from the Turkish sponge *Agelas oroides* that inhibit the enoyl reductases from *Plasmodium falciparum*, *Mycobacterium tuberculosis* and *Escherichia coli*

Deniz Tasdemir,<sup>a,\*</sup> Bülent Topaloglu,<sup>b</sup> Remo Perozzo,<sup>c</sup> Reto Brun,<sup>d</sup> Rosann O'Neill,<sup>e</sup> Néstor M. Carballeira,<sup>e</sup> Xujie Zhang,<sup>f</sup> Peter J. Tonge,<sup>f</sup> Anthony Linden<sup>g</sup> and Peter Ruedi<sup>g</sup>

<sup>a</sup>Centre for Pharmacognosy and Phytotherapy, School of Pharmacy, University of London, London WC1N 1AX, UK

<sup>b</sup>Department of Marine Biology, Faculty of Fisheries, Istanbul University, TR-34480 Istanbul, Turkey

<sup>c</sup>School of Pharmaceutical Sciences, University of Geneva, CH-1211 Geneva 4, Switzerland

<sup>d</sup>Department of Medical Parasitology and Infection Biology, Swiss Tropical Institute, CH-4002 Basel, Switzerland

<sup>e</sup>Department of Chemistry, University of Puerto Rico, Río Piedras, PR 00931-3346, USA

<sup>f</sup>Department of Chemistry, Stony Brook University, NY 11794-3400, USA

<sup>g</sup>Institute of Organic Chemistry, University of Zurich, CH-8057 Zürich, Switzerland

Received 18 May 2007; revised 3 July 2007; accepted 10 July 2007

Available online 22 August 2007

**Abstract**—The type II fatty acid pathway (FAS-II) is a validated target for antimicrobial drug discovery. An activity-guided isolation procedure based on *Plasmodium falciparum* enoyl-ACP reductase (*PfFabI*) enzyme inhibition assay on the *n*-hexane-, the CHCl<sub>3</sub>- and the aq MeOH extracts of the Turkish marine sponge *Agelas oroides* yielded six pure metabolites [24-ethyl-cholest-5 $\alpha$ -7-en-3- $\beta$ -ol (**1**), 4,5-dibromopyrrole-2-carboxylic acid methyl ester (**2**), 4,5-dibromopyrrole-2-carboxylic acid (**3**), (*E*)-oroidin (**4**), 3-amino-1-(2-aminoimidazolyl)-prop-1-ene (**5**), taurine (**6**)] and some minor, complex fatty acid mixtures (**FAMA–FAMG**). **FAMA**, consisting of a 1:2 mixture of (5*Z*,9*Z*)-5,9-tricosadienoic (**7**) and (5*Z*,9*Z*)-5,9-tetracosadienoic (**8**) acids, and **FAMB** composed of **8**, (5*Z*,9*Z*)-5,9-pentacosadienoic (**9**) and (5*Z*,9*Z*)-5,9-hexacosadienoic (**10**) acids in  $\approx$ 3:3:2 ratio were the most active *PfFabI* inhibitory principles of the hexane extract (IC<sub>50</sub> values 0.35  $\mu$ g/ml). (*E*)-Oroidin isolated as free base (**4a**) was identified as the active component of the CHCl<sub>3</sub> extract. Compound **4a** was a more potent *PfFabI* inhibitor (IC<sub>50</sub> 0.30  $\mu$ g/ml = 0.77  $\mu$ M) than the (*E*)-oroidin TFA salt (**4b**), the active and major component of the aq MeOH extract (IC<sub>50</sub> 5.0  $\mu$ g/ml). Enzyme kinetic studies showed **4a** to be an uncompetitive *PfFabI* inhibitor ( $K_i$ : 0.4  $\pm$  0.2 and 0.8  $\pm$  0.2  $\mu$ M with respect to substrate and cofactor). In addition, **FAMA** and **FAMD** (mainly consisting of methyl-branched fatty acids) inhibited *FabI* of *Mycobacterium tuberculosis* (*MtFabI*, IC<sub>50s</sub> 9.4 and 8.2  $\mu$ g/ml, respectively) and *Escherichia coli* (*EcFabI*, IC<sub>50s</sub> 0.5 and 0.07  $\mu$ g/ml, respectively). The majority of the compounds exhibited in vitro antiplasmodial, as well as trypanocidal and leishmanicidal activities without cytotoxicity towards mammalian cells. This study represents the first marine metabolites that inhibit *FabI*, a clinically relevant enzyme target from the FAS-II pathway of several pathogenic microorganisms.

© 2007 Elsevier Ltd. All rights reserved.

## 1. Introduction

Fatty acids (FAs) are essential for all living organisms, because of their key roles in membrane construction and energy production. FAs are synthesized via a repeated cycle of four reactions, condensation, reduction,

dehydration and a final reduction. In mammals and other higher eukaryotes, all these reactions are catalyzed by the type I fatty acid synthase (FAS-I), a large, multi-functional protein.<sup>1</sup> In contrast, bacteria, plants and algae contain a type II system (FAS-II), in which each reaction is carried out by a monofunctional enzyme.<sup>2</sup> The type II fatty acid biosynthesis pathway has recently been discovered in a number of Apicomplexan parasites, including the malaria parasite, *Plasmodium falciparum*.<sup>3</sup> *Mycobacterium tuberculosis* employs both FAS-I and FAS-II systems. FAS-I is responsible for the synthesis of short-chain FAs, whereas the FAS-II system extends

**Keywords:** *Agelas*; Enoyl-ACP reductase; *Plasmodium*; *Mycobacterium*; *Escherichia*.

\* Corresponding author. Tel.: +44 20 7753 5845; fax: +44 20 7753 5909; e-mail: deniz.tasdemir@pharmacy.ac.uk

these FAs for synthesis of very long-chain mycolic acids, which are important components of the mycobacterial cell wall.<sup>4</sup> The central role of FA biosynthesis and the structural differences between the human and microbial FAS systems render FAS-II as an attractive target for antimicrobial drug discovery. The FabI (enoyl-ACP reductase) is a crucial enzyme of all FAS-II systems, since it catalyzes the last NADH-dependent reduction step in each elongation cycle. Several specific FabI inhibitors are known. Triclosan, a broad-spectrum synthetic antibacterial additive in many personal care products such as soaps and toothpastes, is a potent inhibitor of both bacterial and plasmodial FabI.<sup>5–8</sup> Mycobacterial FabI (*Mt*FabI, also called *InhA*) was thought to be the ultimate target for isoniazid, a front-line antitubercular drug,<sup>4</sup> however, recent studies indicate multiple enzyme targets including dihydrofolate reductase.<sup>9,10</sup>

Our research has focused on the plasmodial FAS-II system and the discovery of natural product inhibitors of the individual enzymes in the *Pf*FAS-II cascade. We recently reported the very first antimalarial natural products obtained from endemic Turkish plants that target the *Pf*FabI enzyme.<sup>11,12</sup> Also a number of marine invertebrates collected from Turkish waters were subjected to a target (*Pf*FabI)-based antimalarial screening. The crude methanolic extract of the marine sponge *Agelas oroides* showed promising *Pf*FabI inhibitory and antiplasmodial activity, so it was selected for a more in-depth chemical investigation. Interestingly, a similar enzyme inhibition potential was observed in all *n*-hexane, the CHCl<sub>3</sub> and the aq MeOH-soluble portions of the crude extract. Activity-directed fractionation based on *Pf*FabI inhibition on all three extracts afforded six metabolites (**1–6**) and some complex fatty acid mixtures (**FAMA–FAMG**), which were analyzed by GC–MS after methylation. We undertook mechanistic studies with pure oroidin base (**4a**), the most potent *Pf*FabI inhibitor, and quantitated the ability of this compound to inhibit *Pf*FabI. In addition, all isolates were evaluated for their potency towards FabI of *M. tuberculosis* (*Mt*FabI, *InhA*) and *Escherichia coli* (*Ec*FabI). All marine metabolites were also tested for in vitro antimalarial, leishmanicidal and trypanocidal activities, as well as for cytotoxicity towards mammalian cells to determine their selectivity.

## 2. Results

### 2.1. Extraction, isolation and characterization of the marine metabolites

The crude MeOH extract of *A. oroides* was selected for chemical investigation as it inhibited the recombinant *Pf*FabI protein (IC<sub>50</sub> 20 µg/ml) and concomitantly showed in vitro antimalarial activity (IC<sub>50</sub> 4.4 µg/ml). This extract was subjected to a solvent–solvent partitioning scheme to yield the *n*-hexane, the CHCl<sub>3</sub>- and the aq MeOH-solubles. The partitioning dispersed the bioactivity in all three extracts, which showed IC<sub>50</sub> values of 4.5, 7 and 13 µg/ml towards *Pf*FabI, and 10, 12 and 10 µg/ml towards *P. falciparum*. Hence, each extract

was separately subjected to fractionation, monitored by *Pf*FabI inhibition assay, and their active principles were purified by flash CC (SiO<sub>2</sub>, RP-18) and gel permeation (Sephadex LH20). The isolates were characterized by a combination of 1D/2D-NMR, MS and GC–MS.

The *n*-hexane extract yielded 24-ethyl-cholest-5 $\alpha$ -7-en-3- $\beta$ -ol (**1**) and 4,5-dibromopyrrole-2-carboxylic acid methyl ester (**2**) as major components. The structure of **1** was elucidated by HREIMS, 1D and 2D NMR (including HSQC-TOCSY) and by comparison of its spectroscopic data with previously published values.<sup>13–15</sup> Some of the NMR data were reassigned on the basis of 2D NMR experiments (Table 1). The structure of **2** was readily established on the basis of EIMS, 1D and 2D NMR and by comparison with literature data.<sup>16</sup> Also a number of minor, bioactive FA mixtures (**FAMA–FAMG**) were isolated from the *n*-hexane extract. Due to lack of material, these fractions could not be purified further, but they were analyzed by GC–MS after methylation. Table 3 displays the detailed FA composition of **FAMA–FAMG**. In 1D NMR experiments, **FAMA** seemed to be a pure 5,9-dienoic FA. However, the GC–MS analysis showed it to be a 1:2 mixture of (5*Z*,9*Z*)-5,9-tricosadienoic (23:2, **7**, 36%) and (5*Z*,9*Z*)-5,9-tetracosadienoic acid (24:2, **8**, 64%) methyl esters. Complete NMR data of the mixture **7/8** (**FAMA**, before methylation) that are missing in the literature were assigned by 1D and 2D NMR experiments (Table 1). The GC–MS analysis indicated **FAMB** to be composed of mainly three demospongiac acids, that is, **8** (24:2, 36.3%), (5*Z*,9*Z*)-5,9-pentacosadienoic (25:2, **9**, 33.9%) and (5*Z*,9*Z*)-5,9-hexacosadienoic (26:2, **10**, 19.9%) acids. Based on GC–MS, the most abundant constituent of **FAMC** was 11-methyloctadecanoic acid (11-Me-18:0, 40.3%), followed by stearic (18:0, 13.8%) and oleic acids (18:1 $\Delta^9$ , 9.9%). **FAMD** contained 10-methylhexadecanoic (10-Me-16:0, 21.2%) and palmitic (16:0, 17.9%) acids as major lipids, plus almost equal ( $\geq 6\%$ ) amounts of *ilai*-15:0, *ilai*-17:0, *i*-17:1 $\Delta^9$ , 18:0 and 11-Me-18:0 FAs. **FAME** was rich in oleic (42.3%) and palmitic (16:0, 13.2%) acids, whereas **FAMF** contained five major FAs, oleic (21.7%), 15-methyl-9-hexadecenoic (*i*-17:1 $\Delta^9$ , 16.3%), palmitic (15.1%), 10-methylhexadecanoic (10-Me-16:0, 11.6%) and 16:1 (8.6%) acids. Finally **FAMG** was found to consist of six saturated FAs, with 11-Me-18:0 (38.3%) and phytanic (21.5%) acids being the predominant ones, plus 16:0 (14.8%), 18:0 (12.8%), *ilai*-17:0 (10.3%) and 14:0 (2.3%) (Table 3) (see Fig. 1).

Bioactivity guided purification of the CHCl<sub>3</sub> extract involved C-18 flash and Sephadex LH20 CC to yield **2**, 4,5-dibromopyrrole-2-carboxylic acid (**3a**) and (*E*)-oroidin (**4a**) as the free bases. The <sup>1</sup>H and <sup>13</sup>C NMR spectra of **4a** were very similar to those of the oroidin TFA salt (**4b**), obtained from the aq MeOH extract, which is well described in the literature.<sup>16,17</sup> However, in the <sup>1</sup>H NMR spectrum of **4a** (Table 1, Fig. 2), it was notable that H-9 and H-15 were diamagnetically shifted (approximately –0.3 ppm). Its <sup>13</sup>C NMR spectrum also displayed significant chemical shift differences for C-9, C-10, C-11, C-13 and C-15 (Table 1). The possibility that **4a** could be (*Z*)-oroidin, which has never been isolated from Nature, but

**Table 1.** The NMR data ( $^1\text{H}$  600 MHz,  $^{13}\text{C}$  150 MHz) of FAMA and **1** ( $\text{CDCl}_3$ ), **4a** and **4b** (MeOD)

C	FAMA (7/8)		<b>1</b> <sup>c</sup>		<b>4a</b> <sup>d</sup>		<b>4b</b>	
	$^1\text{H}$	$^{13}\text{C}$	$^1\text{H}$	$^{13}\text{C}$	$^1\text{H}$	$^{13}\text{C}$	$^1\text{H}$	$^{13}\text{C}$
1		180.0 s	1.82 <sup>a</sup> /1.09 <sup>a</sup>	37.4 t				
2	2.36 (t, 7.5)	33.6 t	1.79 <sup>a</sup> /1.39 <sup>a</sup>	31.7 t		128.9 s		128.6 s
3	1.70 (quint., 7.5)	24.8 t	3.60 m	71.3 d	6.82 s	114.4 d	6.85 s	114.4 d
4	2.10 m	26.7 t	1.71 <sup>a</sup> /1.28 <sup>a</sup>	38.4 t		100.0 s		100.0 s
5	5.34 m	128.8 d	1.41 <sup>a</sup>	40.5 d		106.5 s		106.2 s
6	5.36 m	130.8 d	1.76 <sup>a</sup>	29.9 t		161.6 s		161.5 s
7	2.08 m	27.6 t	5.16 m	117.6 d				
8	2.08 m	27.5 t		139.8 s	4.00 (dd, 1.3, 6.1)	42.3 t	4.06 (dd, 1.3, 5.4)	41.5 t
9	5.34 m	129.1 d	1.63 <sup>a</sup>	49.7 d	5.87 (dt, 6.1, 16.0)	121.5 d	6.09 (dt, 5.4, 16.1)	127.7 d
10	5.42 m	130.8 d		34.4 s	6.31 (br d, 16.0)	122.9 d	6.29 (br d, 16.1)	117.6 d
11	2.01 (br q, 6.8)	27.5 t	1.58 <sup>a</sup> /1.46 <sup>a</sup>	21.8 t		131.4 s		126.9 s
12	1.30 <sup>a</sup>	22.9 t	2.02 <sup>a</sup> /1.22 <sup>a</sup>	39.8 t				
13	1.26 (br s)	29.6 t		43.6 s		152.0 s		149.3 s
14	1.26 (br s)	29.6 t	1.80 <sup>a</sup>	55.3 d				
15	1.26 (br s)	29.8 t	1.52 <sup>a</sup> /1.39 <sup>a</sup>	23.2 t	6.47 s	117.7 d	6.72 s	111.7 d
16	1.26 (br s) <sup>b</sup>	29.9 t	1.90 <sup>a</sup> /1.28 <sup>a</sup>	28.2 t				
17	1.26 (br s)	29.9 t	1.22 <sup>a</sup>	56.3 d				
18	1.26 (br s)	29.9 t	0.80 s	13.3 q				
19	1.26 (br s)	29.9 t	0.53 s	12.1 q				
20	1.26 (br s)	29.9 t	1.33 <sup>a</sup>	36.9 d				
21	1.26 (br s)	29.9 t	0.93 (d, 6.6)	19.2 q				
22	1.26 (br s)	32.1 t	1.37 <sup>a</sup> /0.97 <sup>a</sup>	34.1 t				
23	0.88 (t, 7.0)	14.3 q	1.32 <sup>a</sup> /1.05 <sup>a</sup>	26.7 t				
24			0.92 <sup>a</sup>	46.3 d				
25			1.68 <sup>a</sup>	29.2 d				
26			0.82 (d, 6.8)	19.2 q				
27			0.83 (d, 6.8)	19.8 q				
28			1.33 <sup>a</sup> /1.13 <sup>a</sup>	23.2 t				
29			0.86 (t, 7.5)	12.6 q				

All  $\delta$  values are in ppm and  $J$  values (in Hz) are given in parentheses.

<sup>a</sup> Multiplicities are unclear due to overlapping.

<sup>b</sup> In case of **8**, there is an additional  $\text{CH}_2$  group with identical NMR data.

<sup>c</sup> All assignments were based on 2D NMR data (HSQC-TOCSY, HMBC, DQF-COSY).

<sup>d</sup> All assignments were based on 2D NMR data (HSQC, HMBC, DQF-COSY, ROESY).

prepared synthetically,<sup>17</sup> was ruled out due to the large coupling constant of the double bond protons, H-9 and H-10 ( $J_{9,10} = 16.0$  Hz, in (*Z*)-oroidin  $J_{9,10} = 11.5$  Hz<sup>17</sup>). All these differences were indicative of a free (not protonated) imidazole ring, as the NMR data from C-1 through C-8 were identical with those of **4b** (Table 1). To prove this assumption and to support the oroidin skeleton, we undertook a series of 2D NMR experiments. In DQF-COSY spectrum, H-8 scalarly coupled with H-9, which in turn coupled with H-10. HMBC correlations observed between C-8/H-9, C-8/H-10, C-9/H<sub>2</sub>-8, C-9/H-10; C-10/H<sub>2</sub>-8, C-10/H-15; C-11/H<sub>2</sub>-8, C-11/H-9, C-11/H-10, C-11/H-15; C-13/H-15 and ROE couplings between H-8/H-9, H-8/H-10, H-9/H-10 and H-9/H-15 led to the assignments of the remaining resonances (C-9 through C-15). Upon addition of TFA-*d*, compound **4a** was immediately converted to **4b** (Fig. 2). Recently, the oroidin sodium salt was described from *Axinella damicornis* with the identical  $^1\text{H}$  NMR data as **4a**, but the published  $^{13}\text{C}$  NMR data remained incomplete.<sup>18</sup> This compound gave  $[\text{M}+22]^+$  peaks in the (+)-ESI-MS spectrum ( $m/z$  410, 412 and 414, 1:2:1). However, the (+)-ESI-MS spectrum of **4a** was lacking these peaks, and only the typical  $[\text{M}+\text{H}]^+$  peaks at  $m/z$  388, 390 and 392 (1:2:1) were present. Hence, we rule out that our **4a** is

the oroidin Na salt, instead it must be the free (*E*)-oroidin base.

The aq MeOH extract was also prefractionated as described above (C-18 flash CC). However, due to use of solvents containing TFA (0.1%), the metabolites 4,5-dibromopyrrole-2-carboxylic acid (**3b**), oroidin (**4b**), **5** and taurine (**6**) were isolated as either TFA salts or TFA adducts. The structure of **5** was easily identified as 3-amino-1-(2-aminoimidazolyl)-prop-1-ene by spectroscopic means (1D NMR, ESIMS) and by comparison with literature data.<sup>19</sup> Taurine (**6**) had only two aliphatic  $\text{CH}_2$  signals, in both the  $^1\text{H}$  and the  $^{13}\text{C}$  NMR spectra, and no carbonyl signal. Its molecular weight was determined to be  $m/z$  125 by negative mode ESIMS ( $m/z$  124  $[\text{M}-\text{H}]^-$ , 249  $[2\text{M}-\text{H}]^-$ ). As only limited information could be gathered from NMR spectroscopy, the structure elucidation of **6** was resolved by an X-ray diffraction analysis, which revealed the same structure as those reported previously for taurine, which is also known as 2-aminoethane sulfonic acid or  $\beta$ -alanine sulfonic acid.<sup>20–23</sup> Two additional taurine-like compounds with only two  $\text{CH}_2$  signals in both the  $^1\text{H}$  and the  $^{13}\text{C}$  NMR spectra were also isolated. However, as they did not produce good quality single crystals in common solvents, their structures remain unresolved.

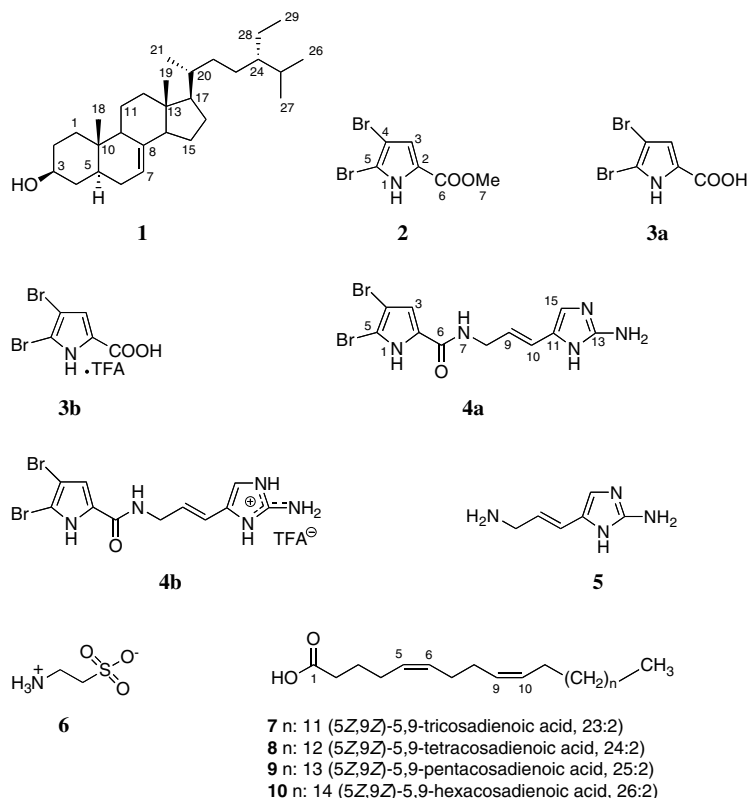


Figure 1. The chemical structures of *Agelas oroides* metabolites.

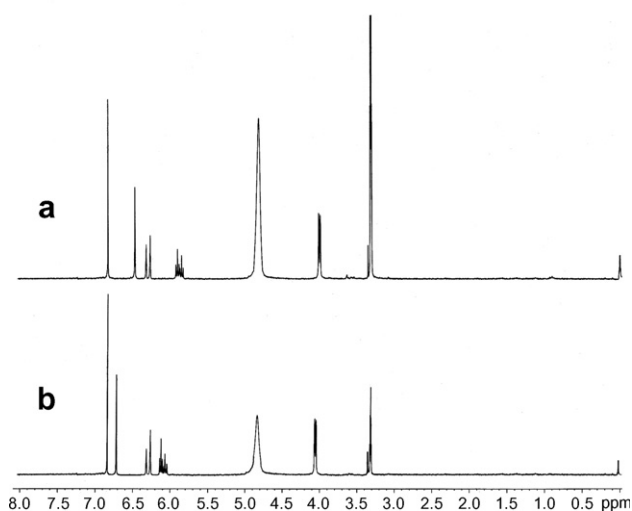


Figure 2. The  $^1\text{H}$  NMR spectrum of (a) oroidin base (**4a**); (b) oroidin TFA salt (**4b**) formed after addition of one drop of TFA-*d* (300 MHz, MeOD).

## 2.2. Inhibitory activity towards *Pf*FabI

The ability of crude extracts, pure compounds, as well as the FA mixtures to inhibit the recombinant *Pf*FabI enzyme was investigated by a spectrophotometric method (Table 2). Among the metabolites obtained from the *n*-hexane extract, **FAMA** and **FAMB** exerted the highest inhibitory potential with  $\text{IC}_{50}$  value of  $0.35 \mu\text{g}/\text{ml}$ . Notably, both are mixtures of two or three diunsaturated

FAs, respectively (Table 3). The second most active FA mixtures were **FAME** and **FAMF** ( $\text{IC}_{50}$   $0.65 \mu\text{g}/\text{ml}$  for both). **FAME** was dominated by the monounsaturated oleic acid ( $18:1\Delta^9$ ) and contained considerable amounts (16.6%) of the 5,9-dienoic acids, **7/8**. **FAMF** also contained the monounsaturated FAs ( $18:1\Delta^9$ ,  $i-17:1\Delta^9$ ), plus several saturated acids. **FAMC**, which had a higher portion of unsaturated fatty acids than **FAMD**, has a better enzyme inhibitory activity ( $\text{IC}_{50}$ s 1.0 and  $2.5 \mu\text{g}/\text{ml}$ , respectively). **FAMG** contains only saturated FAs, including the isoprenoid-like FA phytanic acid, and exhibits the weakest *Pf*FabI inhibitory potential ( $\text{IC}_{50}$   $20 \mu\text{g}/\text{ml}$ ). Since the major metabolites **1** ( $\text{IC}_{50}$   $18 \mu\text{g}/\text{ml}$ ) and **2** ( $\text{IC}_{50}$   $> 100 \mu\text{g}/\text{ml}$ ) possessed moderate or no *Pf*FabI inhibiting activity, the FA mixtures, in particular those rich in mono- and diunsaturated FAs, appear as the active principles of the *n*-hexane extract.

In contrast to **2** and **3a**, which did not maintain the initial bioactivity of the C-18 fractions from the  $\text{CHCl}_3$  extract, oroidin base (**4a**) retained the potent enzyme inhibitory activity with an  $\text{IC}_{50}$  value of  $0.30 \mu\text{g}/\text{ml}$  ( $=0.77 \mu\text{M}$ ). Oroidin TFA salt (**4b**) was the major and the most active *Pf*FabI inhibitory principle of the aq MeOH extract ( $\text{IC}_{50}$   $5 \mu\text{g}/\text{ml} = 12.8 \mu\text{M}$ ). Interestingly, **3b**, but not **3a**, had some weak *Pf*FabI inhibiting activity ( $\text{IC}_{50}$   $40 \mu\text{g}/\text{ml}$ ). Compounds **5** and **6** were inactive.

## 2.3. *Pf*FabI enzyme kinetics for **4a**

Due to the potent inhibition of *Pf*FabI by **4a**, kinetic parameters were determined to elucidate its binding

**Table 2.** The *Pf*FabI inhibitory and antiprotozoal activities of the extracts and isolated components of *Agelas oroides* sponge (IC<sub>50</sub> values are in µg/ml, <sup>a</sup>triclosan, <sup>b</sup>artemisinin, <sup>c</sup>melarsoprol, <sup>d</sup>benznidazole, <sup>e</sup>miltefosine, <sup>f</sup>podophyllotoxin)

Sample	<i>Pf</i> FabI inhibition	<i>P. falciparum</i>	<i>T. brucei rhodesiense</i>	<i>T. cruzi</i>	<i>L. donovani</i>	L6 cell cytotox.
Standard	0.014 <sup>a</sup>	0.0045 <sup>b</sup>	0.0027 <sup>c</sup>	0.17 <sup>d</sup>	0.12 <sup>e</sup>	0.009 <sup>f</sup>
Crude MeOH ext.	20	4.4	3.8	24.3	11.4	15.9
<i>n</i> -Hexane ext.	4.5	10	90	>30	30	>90
CHCl <sub>3</sub> ext.	7.0	12	27.6	>30	20	>90
Aq MeOH ext.	13.0	10	48.4	>30	30	15.7
<b>FAMA</b>	0.35	12.1	12.0	>30	11.4	83.6
<b>FAMB</b>	0.35	16.3	10.1	>30	14.4	84.7
<b>FAMC</b>	1.0	11.5	9.9	>30	10	86.4
<b>FAMD</b>	2.5	40.9	42.3	>30	9.8	>90
<b>FAME</b>	0.65	3.4	5.3	>30	9.0	59.8
<b>FAMF</b>	0.65	8.7	5.7	>30	6.0	43.2
<b>FAMG</b>	20	17.8	14.0	16	11.9	38.5
<b>1</b>	18	16.1	14.2	>30	29.5	>90
<b>2</b>	>100	>50	13.3	>30	>30	>90
<b>3a</b>	>100	>50	20.9	>30	7.9	>90
<b>3b</b>	40	49.9	25.2	>30	5.8	>90
<b>4a</b>	0.30	3.9	17.3	>30	>30	88.6
<b>4b</b>	5.0	7.9	12.2	>30	15.4	76.4
<b>5</b>	>100	7.4	2.4	2.5	13.1	0.7
<b>6</b>	>100	>50	83.4	>30	>30	>90

mechanism. It was identified as an uncompetitive inhibitor of *Pf*FabI with respect to crotonoyl-CoA and NADH (Fig. 3). The Dixon plot analysis provides  $K_i$  values of  $0.4 \pm 0.2 \mu\text{M}$  when varying the crotonoyl-CoA concentration and  $0.8 \pm 0.2 \mu\text{M}$  when varying the NADH concentration.

#### 2.4. In vitro antiplasmodial activity against K1 strain of *Plasmodium falciparum*

All crude extracts, pure compounds and the FA mixtures were assayed for their in vitro inhibitory activity on multidrug resistant K1 strain of *P. falciparum*. Generally, the antiplasmodial potential was well correlated with *Pf*FabI enzyme inhibitory activity. Two potent *Pf*FabI inhibitory FA mixtures **FAME** and **FAMF** emerged to be very active in whole cell assays (IC<sub>50</sub>s 3.4 and 8.7 µg/ml, respectively). **FAMA** and **FAMB**, the most potent *Pf*FabI inhibitors of the *n*-hexane extract, exerted slightly lower potency (IC<sub>50</sub>s 12.1 and 16.3 µg/ml). The antiparasitic efficacy of **FAMC** and **FAMD** was also moderate (IC<sub>50</sub>s 11.5 and 40.9 µg/ml). The steroid **1** and **FAMG** inhibited the cultures of malaria parasite with the same efficacy as their enzyme inhibiting activity (Table 2).

Oroidin base (**4a**), the most potent *Pf*FabI inhibitor, exhibited an IC<sub>50</sub> value of 3.9 µg/ml in the whole cell parasite assays. This activity was greater than that of the oroidin TFA salt **4b** (IC<sub>50</sub> 7.9 µg/ml). The ability of **3b** to inhibit *P. falciparum* cultures (IC<sub>50</sub> 49.9 µg/ml) was as weak as its *Pf*FabI enzyme inhibitory effect. Inactive were **2**, **3a** and **6** (IC<sub>50</sub> > 50 µg/ml), whereas **5** had appreciable antiplasmodial activity with an IC<sub>50</sub> value of 7.4 µg/ml. None of these compounds inhibited *Pf*FabI.

#### 2.5. *Mt*FabI (InhA) and *Ec*FabI inhibitory activities

All marine isolates were tested against the analogous FabI enzymes from *M. tuberculosis* (*Mt*FabI, InhA)

and *E. coli* (*Ec*FabI). Except for **FAMA** and **FAMD**, all metabolites were inactive at the highest concentrations tested (IC<sub>50</sub>s > 50–100 µg/ml). The inhibitory activity of **FAMA** and **FAMD** on *Mt*FabI was moderate (IC<sub>50</sub>s 9.4 and 8.2 µg/ml, respectively), but both were very potent against *Ec*FabI with IC<sub>50</sub> values of 0.50 µg/ml (**FAMA**) and 0.07 µg/ml (**FAMD**). Table 4 compares the inhibitory effects of these fractions against all three FabI enzymes. Due to very low available amounts of **FAMA** and **FAMD**, we were not able to evaluate their ability to inhibit the growth of *M. tuberculosis* and *E. coli* cultures.

#### 2.6. Trypanocidal, leishmanicidal and cytotoxic potential of the isolates

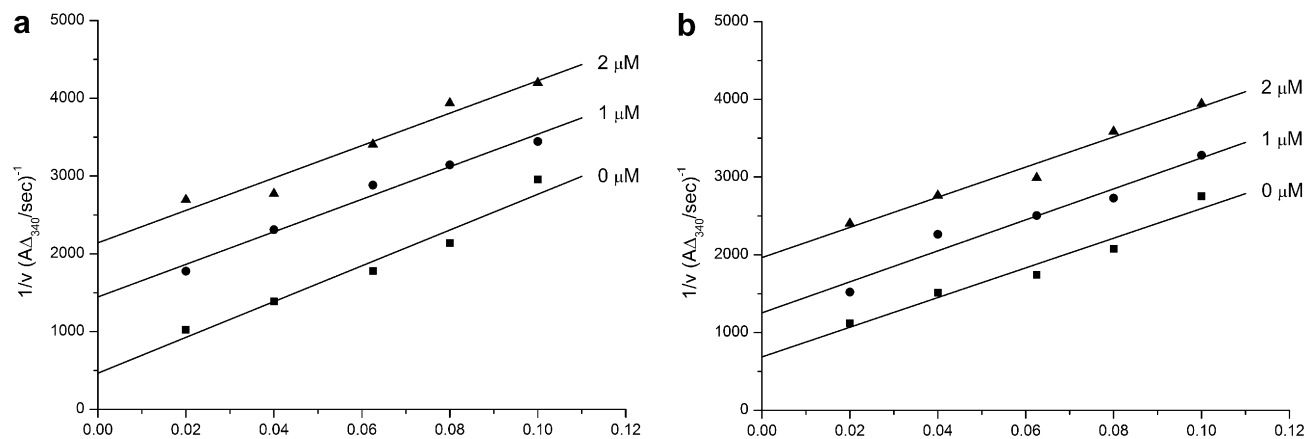
The crude extracts and the marine metabolites were also evaluated towards other parasitic protozoa, that is, *Trypanosoma brucei rhodesiense*, *T. cruzi* and *Leishmania donovani* (Table 2). Blood-stream life cycle forms of cultured parasites, which are the clinically most relevant forms, were used for the assays. All compounds showed activity against African *T. brucei rhodesiense*, with **5** being the most potent one (IC<sub>50</sub> 2.4 µg/ml). Among the FA mixtures, **FAME** and **FAMF** displayed the highest (IC<sub>50</sub>s 5.3 and 5.7 µg/ml), and **FAMD** the least (IC<sub>50</sub> 42.3 µg/ml) antitrypanosomal activity. Overall, the lowest activity against this parasite was exerted by taurine (**6**, IC<sub>50</sub> 83.4 µg/ml). In contrast, only two isolates, **5** and **FAMG**, showed some potential against the American trypanosome, *T. cruzi*. Notably, the potency of compound **5** was identical (IC<sub>50</sub> 2.5 µg/ml) to that observed for African trypanosomes. **FAMG** exhibited much lower activity (IC<sub>50</sub> 16 µg/ml). The majority of the compounds possessed inhibitory effects on axenic *L. donovani* amastigotes. It is noteworthy that **4a** was inactive at the highest tested concentration, whereas **4b** had a moderate leishmanicidal effect (IC<sub>50</sub> 15.4 µg/ml). In contrast, **3a** and **3b** were almost equipotent (IC<sub>50</sub>s 7.9 and 5.8 µg/ml, respectively). Again, all FA mixtures

**Table 3.** The fatty acid composition of bioactive FAMA–FAMG mixtures determined by GC–MS (% from the total methylated FAs)

FA	FAMA	FAMB	FAMC	FAMD	FAME	FAMF	FAMG
<i>n</i> -14:0		0.2	0.6	1.7	3.0	0.6	2.3
<i>i</i> -14:0				0.2			
<i>n</i> -15:0		0.4	0.6	0.8			
br-15:0				0.2			
<i>ilai</i> -15:0				<b>8.0</b>	1.2	1.0	
<i>n</i> -16:0		0.6	3.7	<b>17.9</b>	<b>13.2</b>	<b>15.1</b>	<b>14.8</b>
br-16:0				0.7		0.5	
<i>ilai</i> -16:0				3.2			
16:1		0.2	1.1	3.5	2.0	<b>8.6</b>	
<i>n</i> -17:0		0.4	0.4	1.8	0.7	1.3	
br-17:0				2.6			
10-Me-16:0				<b>21.2</b>	0.9	<b>11.6</b>	
<i>ilai</i> -17:0			3.9	<b>7.6</b>		3.8	<b>10.3</b>
17:1				3.6			
br-17:1					0.5		
<i>i</i> -17:1 $\Delta^9$				<b>6.9</b>		<b>16.3</b>	
<i>i</i> -17:2 $\Delta^{5,9}$						1.8	
<i>n</i> -18:0		0.6	<b>13.8</b>	<b>6.3</b>	5.5	5.8	<b>12.8</b>
br-18:0				0.7			
18:1 $\Delta^{11}$			3.9	2.1	2.7	5.6	
18:1 $\Delta^9$		2.9	<b>9.9</b>	2.6	<b>42.3</b>	<b>21.7</b>	
18:2 $\Delta^{9,12}$			1.3		1.8	1.5	
18:2 $\Delta^{5,9}$				0.8			
11-Me-18:0			<b>40.3</b>	<b>6.5</b>	3.2	4.5	<b>38.3</b>
<i>n</i> -19:0			0.9	0.1			
19:1			2.6	1.0			
br-19:1			3.0				
br-20:0							<b>21.5*</b>
20:1			3.2				
20:2 $\Delta^{5,9}$			5.2		1.4	0.3	
<i>n</i> -21:0			2.4				
21:2 $\Delta^{5,9}$			1.1				
<i>n</i> -22:0					0.9		
22:2 $\Delta^{5,9}$		0.8					
<i>n</i> -23:0			0.6		1.4		
23:1		0.6					
23:2 $\Delta^{5,9}$	<b>36</b>	1.6					
24:1		1.0					
24:2 $\Delta^{5,9}$	<b>64</b>	<b>36.3</b>	1.5		<b>9.1</b>		
25:2 $\Delta^{5,9}$		<b>33.9</b>			<b>7.5</b>		
26:2 $\Delta^{5,9}$		<b>19.9</b>			2.7		

The major fatty acids are shown bold.

br, methyl-branched, position not determined; *i*, *iso* methyl-branched; *ai*, *anteiso* methyl-branched; unless indicated with  $\Delta$ , the position of double bond(s) not determined. \*, Phytanic acid.

**Figure 3.** Enzyme kinetics of **4a** (a) while crotonoyl-CoA is varied; (b) while NADH is varied.

**Table 4.** IC<sub>50</sub> values (µg/ml) of FAMA, FAMB and FAMD against FabI enzymes of different origin

Fatty acid	<i>Pf</i> FabI	<i>Ec</i> FabI	<i>Mt</i> FabI
<b>FAMA</b>	0.35	0.50	9.4
<b>FAMB</b>	0.35	>50	>50
<b>FAMD</b>	2.5	0.070	8.2

exerted moderate to good antileishmanial effects (IC<sub>50</sub>s from 6.0 to 14.4 µg/ml). The steroid **1** was the weakest metabolite (IC<sub>50</sub> 29.5 µg/ml) towards *L. donovani* amastigotes, whereas **2** and **6** were completely inactive.

The isolates have simultaneously been tested on primary mammalian (rat skeletal myoblast) L6 cells, in order to determine their therapeutic (selectivity) index. Compound **5** appeared to be the only metabolite with strong cytotoxicity on L6 cells with an IC<sub>50</sub> value of 0.7 µg/ml. The similar activity profile towards all parasites tested as well as the cytotoxicity on mammalian L6 cells indicates that **5** is a toxic compound with a very low therapeutic index. The remaining compounds were, however, either weakly cytotoxic, or were devoid of any cytotoxicity (Table 2).

### 3. Discussion

*Agelas oroides* is a common marine sponge, well known for producing a vast diversity of pyrrole and imidazole alkaloids. Of the 90 pyrrole–imidazole alkaloids known so far, 60 have been isolated from *Agelas* species.<sup>24,25</sup> Oroidin, the most abundant member of this class, is believed to be the common biogenetic precursor of many precedented and unprecedented pyrrole–imidazole alkaloids.<sup>24–26</sup> The biogenesis of oroidin itself has been postulated to be via condensation of compounds **3** and **5**.<sup>19,24,27</sup> This is supported by the co-occurrence of these compounds in two morphologically and chemically indistinguishable Axinellid sponges, *Teichaxinella morchella* and *Ptilocaulis walpersi*.<sup>19</sup> To our knowledge, this is the first study reporting the occurrence of **3** and **5** together in an *Agelas* sponge. In addition, this is only the second report of **5** from natural sources. It is likely that this metabolite escaped isolation by marine chemists due to its high polarity.

Since *Agelas* species are rich in Δ<sup>5</sup>- and Δ<sup>7</sup>-stanols, the presence of **1**, a cholestenol, as the predominant steroidal constituent of *A. oroides* is in accordance with previous data.<sup>14,28</sup> Marine sponges possess unique biomembranes, which contain unusual fatty acids, for example, the very long chain (≥C20) demospongiac FAs. Such FAs with unsaturation(s) at C-5 and C-9 are common in *Agelas* sp. Some unusual ethylene-interrupted Δ<sup>5,9</sup>-dienoic acids have been thought to arise from a symbiotic relationship.<sup>29</sup> The presence of phytanic acid, which originates from phytol, a constituent of the chlorophyll molecule,<sup>30</sup> in good quantities in FAMG might give further evidence for the contribution of the symbiotic organisms to the fatty acid profile of *A. oroides*. Taurine (**6**) is an important neurotransmitter in vertebrates and has repeatedly been found in many marine invertebrates, for example, hydrozoans,<sup>31</sup> starfish and sponges.<sup>32</sup> Taurine conjugated

FAs have been isolated from *Ircinia*<sup>33,34</sup> and *Hippospongia* sponges.<sup>35</sup> Oroidin-like compounds possessing a taurine residue have also been reported from several sponge genera, for example, *Hymeniacion*,<sup>36</sup> *Acanthella*<sup>37</sup> and *Agelas*.<sup>38,39</sup> To the best of our knowledge, this is the first report of taurine in a free form from the genus *Agelas*.

We previously reported the very first natural inhibitors of *Pf*FabI from endemic Turkish plants.<sup>11,12</sup> We have now expanded our studies into marine organisms and, based on the activity in the preliminary screening, we have worked up the *n*-hexane, the CHCl<sub>3</sub> and the aq MeOH extracts of the marine sponge *A. oroides*. Oroidin base (**4a**) appeared as the most potent *Pf*FabI inhibitory principle of the *Agelas* sponge. The kinetic analysis revealed an uncompetitive binding mechanism with respect to substrate and cofactor, indicating that **4a** is exclusively binding to the enzyme–substrate complex or enzyme–cofactor complex. This mechanism is identical to the one observed for triclosan towards FabI of various species.<sup>40,41</sup> The TFA salt of oroidin (**4b**) was also active against *Pf*FabI, but there is a significant decrease of activity (almost 20-fold) in comparison with **4a**. At this point it is difficult to explain the reason underlying this difference. On one hand, assuming that TFA would form stable ion pairs with **4a**, one could assume that the alkaloid/TFA complex becomes too big to bind at the relevant enzyme-binding site when compared with the free base. In addition, the alkaloid salt is charged and its interaction with the enzyme may thus be disturbed. The results of ongoing crystallographic studies will help to answer this question. On the other hand, the pH of the target site for an antimalarial agent is very important. A well-known example is chloroquine, a weakly basic compound. The erythrocyte and parasite membranes are freely permeable to the uncharged chloroquine, but the drug gets trapped in the acidic digestive vacuole upon protonation, and accumulates in very high concentrations.<sup>42,43</sup> A similar scenario may be assumed for oroidin (**4a**), thus resulting in improved growth inhibitory effect against *P. falciparum* whole cells compared with **4b**. It would be very important to know the pH of the apicoplast, the organelle where FA synthesis takes place.

It has previously been observed that the *Agelas* sponges are not fed on by predatory reef fish, and oroidin was identified as major feeding-deterrent agent.<sup>44</sup> Current knowledge indicates that the pyrrole portion (**3**) of oroidin is required for deterring activity, but **3** is not sufficiently active itself. The imidazole portion (**5**) has no protective effect on its own, but enhances the activity of the pyrrole part.<sup>25,44</sup> A similar structure–activity–relationship can be observed for inhibition of *Pf*FabI. The imidazole portion of the molecule appears to have no effect on *Pf*FabI, but has an unspecific (toxic) effect on the malaria parasite. Compound **3** is not toxic, but has limited antimalarial and *Pf*FabI inhibition activities. In contrast, their condensation product, that is, oroidin, has excellent *Pf*FabI inhibition and also antimalarial potential without significant cytotoxicity. Interestingly, König et al. previously reported oroidin (TFA salt) to be inactive towards the D6 and W2 strains of *P. falciparum*.

rum.<sup>16</sup> However, a very recent study reported its antimalarial effect with an IC<sub>50</sub> value of 1.2 µg/ml.<sup>45</sup> This is in line with our results, although a different strain (D6) was used. The same group reported only marginal activity of oroidin towards *M. tuberculosis*.<sup>45</sup> Although oroidin acts as an antifouling agent in the sponge and inhibits marine bacteria found in seawater at natural concentrations,<sup>46</sup> it was found to be inactive against a number of Gram-positive and Gram-negative human pathogenic bacteria.<sup>45</sup> These findings indirectly support our results, in which oroidin failed to interact with the *MtFabI* and *EcFabI* enzymes. It is noteworthy that neither oroidin, nor other FabI inhibitory compounds have toxicity on mammalian L6 cells. The only exception is compound **5**, which has no FabI inhibition potential.

An intriguing result emerging from this study was the moderate to very potent *PfFabI* enzyme inhibitory activity of complex inseparable FA mixtures. The *PfFabI* inhibitory activity of the FA mixtures appeared to be related to their unsaturation levels, that is, FA mixtures rich in mono- and diunsaturated FAs (**FAMA**, **FAMB**, **FAME**, **FAMF**) inhibited *PfFabI* more efficiently. This trend seemed to be valid for the remaining FA mixtures with lower IC<sub>50</sub> values. However, the chain length of the FAs seemed to be less crucial for *PfFabI* inhibition, as the activity of **FAMA** and **FAMB** containing very long chain FAs (C<sub>23</sub>–C<sub>26</sub>) was comparable with that of **FAME** and **FAMF**, which are dominated by shorter FAs (C<sub>16</sub>–C<sub>18</sub>). More importantly, the enzyme inhibition generally correlated with the antiplasmodial effects of the compounds in whole cell assays. The FA mixtures rich in shorter monounsaturated fatty acids (**FAME**, **FAMF**) had greater antimalarial potential compared to those rich in dienoic acids. The only one exception was **FAMG**, which consisted of phytanic acid and mainly saturated FAs, which had equal IC<sub>50</sub> values towards both *PfFabI* and the malaria whole cells. Interestingly, **FAMA** and **FAMD** were the only fractions that inhibited *MtFabI* (InhA) and *EcFabI*. **FAMA** was very potent towards both *EcFabI* and *PfFabI*, but was less active against *MtFabI*. It was somewhat surprising that **FAMA**, consisting of a 1:2 mixture of 5,9-23:2 (**7**) and 5,9-24:2 (**8**) demospongiic acids, was active against both *MtFabI* and *EcFabI*, whereas **FAMB** consisting of a 3:3:2 mixture of 5,9-24:2 (**8**), 5,9-25:2 (**9**) and 5,9-26:2 (**10**) was inactive (Table 4). This suggests that (5*Z*,9*Z*)-5,9-tricosadienoic acid (**7**) is the active component in **FAMA** that inhibits *EcFabI* and *MtFabI*. Interestingly, **FAMD**, which is rich in shorter, methyl-branched saturated FAs (C<sub>16</sub>–C<sub>19</sub>), is even more potent against *EcFabI* than **FAMA**. This observation is consistent with the known substrate specificity of *EcFabI*, which elongates FAs up to a chain length of C-18. In contrast, **FAMA** and **FAMD** had similar activities against *MtFabI*, which is perhaps surprising given the fact that this enzyme is involved in the biosynthesis of very long chain length (>C<sub>50</sub>) FAs.<sup>47</sup>

#### 4. Conclusions

The FAS-II pathway is a validated target for antimicrobial drug discovery. In bacteria, this pathway is carried

out in the cytoplasm, whereas in *P. falciparum*, it is localized in the apicoplast, a plastid-like organelle ancestrally related to cyanobacteria.<sup>48</sup> Due to the prokaryotic nature of the apicoplast, its metabolic machinery differs from that of the mammalian host. Type II FAS is carried out by a set of individual enzymes in conjunction with acyl carrier protein (ACP)-associated substrates. *FabI* catalyzes the final step of the chain elongation process, and thus is an excellent target for malaria research. Herein we described the first antimalarial marine natural products that target *PfFabI*. Oroidin (**4a**) emerged as a potent and selective inhibitor of *PfFabI*, as it did not inhibit *MtFabI* or *EcFabI* homologues. Due to the correlation between the enzyme inhibition and the antiplasmodial activity, oroidin represents a promising lead compound.

Another intriguing finding from this study is the differential activity of **FAMA** and **FAMD** against various enoyl-ACP reductases. **FAMA** equipotently inhibits *EcFabI* and *PfFabI*, but is less active against *MtFabI*. This is consistent with a recent study in which it was shown that long chain unsaturated FAs inhibit the *FabI* enzyme from several species of bacteria and show antibacterial activity.<sup>49</sup> In contrast to **FAMA**, **FAMD** is an excellent inhibitor of *EcFabI* while having only limited activity against *MtFabI* and *PfFabI*. This indicates that shorter, methyl-branched saturated FAs (C<sub>16</sub>–C<sub>19</sub>) selectively inhibit *EcFabI*. Given that saturated FAs were shown to be inactive in the studies conducted by Zheng et al. (IC<sub>50s</sub> > 2 mM),<sup>49</sup> our observation suggests that branching is important for activity against *EcFabI*. Thus, our study is the first report that marine-derived long chain unsaturated and short methyl-branched saturated FAs are selective inhibitors of the bacterial *FabI* enzyme. This does not appear to be an unspecific enzyme inhibitory effect, because in that case all three enoyl-ACP reductases would be inhibited by all FA mixtures. While antimalarial effects of some unsaturated FAs have previously been described,<sup>50</sup> their mechanism of action has so far remained undetermined. We are currently undertaking further studies to synthesize individual FAs in order to better understand their mechanism of action towards enoyl-ACP reductases and to evaluate their antibacterial and antiplasmodial effect.

## 5. Experimental

### 5.1. General procedures

Optical rotations were measured at 23 °C on a Perkin–Elmer 241 MC polarimeter using Na lamp (589 nm). The routine <sup>1</sup>H NMR spectra were obtained on a Bruker ARX 300 MHz instrument, whereas <sup>13</sup>C-, DEPT-135 and 2D-NMR spectra were acquired on a Bruker DRX spectrometer operating at 600 (<sup>1</sup>H NMR) and 150 (<sup>13</sup>C NMR) MHz. The chemical shift values are reported as parts per million (ppm) units relative to tetramethylsilane (TMS). ESI-mass spectra were taken on a Bruker Esquire-LC–MS (ESI mode) spectrometer, while EIMS analyses were performed on a Finnigan MAT95

(70 eV) spectrometer. Enzyme assays were performed using a Cary 300 Bio (Varian) spectrophotometer. SiO<sub>2</sub> 60 (40–63 μm, Merck) and RP-18 (40–63 μm, LiChroprep 18) materials were used for Flash CC separations. Sephadex LH20 was purchased from Amersham Biosciences (Uppsala, Sweden). TLC analyses were carried out on precoated silica gel 60 F<sub>254</sub> (Merck) TLC plates.

## 5.2. Animal material

The sponge material was collected in June 2002 using SCUBA (–10 m) in Gökçeada (Northern Aegean Sea, Turkey). The animal material was kept frozen until work-up. A taxonomic voucher specimen (sample # GA02-01-05) is maintained at the University of London, School of Pharmacy.

## 5.3. Extraction and isolation

The sponge material was homogenized by a household mixer and extracted successively with MeOH, MeOH/CHCl<sub>3</sub> (1:1) and CHCl<sub>3</sub>. The filtered solutions were combined and evaporated to dryness at 30 °C to yield 6.93 g of crude, orange-brown gum. This material was suspended in MeOH/H<sub>2</sub>O mixture (9:1, 200 ml) and partitioned against *n*-hexane (3 × 200 mL). The aqueous layer was then diluted to 70% MeOH (v/v) with H<sub>2</sub>O and partitioned against CHCl<sub>3</sub> (3 × 200 mL). All extracts were separately evaporated to dryness under vacuum and yielded 1.06 g (*n*-hexane), 1.08 g (CHCl<sub>3</sub>) and 3.46 g (aq MeOH) of material.

The *n*-hexane extract was fractionated on a SiO<sub>2</sub> flash column (100 g) using gradient amounts of EtOAc (0–100%) in hexane to afford 13 fractions. The activity was detected in fractions 4–9. A precipitate, mainly consisting of impure **2** (30 mg), occurred during the work-up of fraction 4. It was removed by filtration, then, the hexane soluble part of this fraction (60 mg) was submitted to Sephadex LH20 column chromatography (CC) employing CHCl<sub>3</sub> as eluent to yield 18 mg of **1** and 4 mg of **FAMA**. The most active fraction 5 (33 mg) was also applied to a Sephadex (CHCl<sub>3</sub>) column to furnish **FAMB** (4.1 mg), **FAMC** (2.9 mg) and another fraction (6.7 mg). The latter was chromatographed over a gravity-driven SiO<sub>2</sub> column (hexane/EtOAc 95:5 to 80:20) to give **FAMD** (3.7 mg). Due to similarities by TLC and <sup>1</sup>H NMR, the active fractions 6 and 7 were combined (17 mg) and also passed through a Sephadex LH20 column (CHCl<sub>3</sub>) to yield **FAME** (4 mg) and **FAMF** (2.6 mg). Finally, moderately active fractions 8 and 9 were combined and separated in the same fashion to afford **FAMG** (2.4 mg).

The active CHCl<sub>3</sub> extract was fractionated on a C-18 flash column using a 10% stepwise gradient from 100% H<sub>2</sub>O to 100% MeOH. The *Pf*FabI inhibitory activity was tracked to three fractions, that is, the combined fractions 3–6 (25 mg), 7–8a (70 mg) and 8b–9b (176.9 mg). The weakly active fractions 3–6 were purified over a Sephadex LH20 column (MeOH) to yield **3a** (6.9 mg). The very active fraction 7–8a was also puri-

fied the same way to furnish oroidin base (**4a**, 5 mg). The purification of the final fraction 8b–9b over the same column gave **2** (114 mg).

The aq MeOH extract was also fractionated over a C-18 flash column using a 10% stepwise gradient from 100% aq TFA (0.1%) to 100% MeOH. This afforded eleven fractions (0–10). The fractions 0–1 were combined and submitted to Sephadex LH20 CC (70% MeOH in H<sub>2</sub>O) to give 47 fractions. During the evaporation of the fractions 21–22 (161 mg) and 23–24 (7.7 mg) some precipitates appeared, which were combined and resubjected to gel chromatography (Sephadex LH20, MeOH) to elaborate taurine (**6**, 8 mg). The soluble portion of the fractions 21–22 was similarly chromatographed to yield **5** (35 mg) and two unidentified taurine-like compounds (9.3 mg and 10.9 mg). The purification of the most active C-18 fractions 7–8 (410 mg) and 9 (216 mg) was also achieved by Sephadex LH20 CC (MeOH) to give the oroidin TFA salt (**4b**, 213 mg) and the 4,5-dibromopyrrole-2-carboxylic acid TFA adduct (**3b**, 60 mg), respectively.

**5.3.1. 24-Ethyl-cholest-5 $\alpha$ -7-en-3- $\beta$ -ol (1).** [ $\alpha$ ]<sub>D</sub> +10.6 (23 °C, *c* = 0.7). EIMS (*m/z*, relative intensity) 414 ([M]<sup>+</sup>, 100). HREIMS *m/z* 414.3856 (Calcd for C<sub>29</sub>H<sub>50</sub>O 414.3862). <sup>1</sup>H NMR (CDCl<sub>3</sub>, 600 MHz) and <sup>13</sup>C NMR (CDCl<sub>3</sub>, 150 MHz), see Table 1.

**5.3.2. 4,5-Dibromopyrrole-2-carboxylic acid methyl ester (2).** EIMS (*m/z*, relative intensity) 281/283/285 (M<sup>+</sup>, 36/68/35), 249/251/253 (52/100/50). (–)-ESIMS *m/z* 280/282/284 (M–H<sup>+</sup>, 1/2/1). <sup>1</sup>H NMR (300 MHz, MeOD)  $\delta$  6.84 (s, H-3), 3.82 (3H, s, H<sub>3</sub>-7). <sup>1</sup>H NMR (300 MHz, CDCl<sub>3</sub>)  $\delta$  10.1 (br s, NH-1), 6.91 (d, *J* = 2.0 Hz, H-3), 3.90 (3H, s, CH<sub>3</sub>-7). <sup>13</sup>C NMR (75 MHz, MeOD):  $\delta$  125.2 (s, C-2), 118.6 (d, C-3), 100.5 (s, C-4), 107.9 (s, C-5), 161.2 (s, C-6), 52.0 (q, C-7).

**5.3.3. 4,5-Dibromopyrrole-2-carboxylic acid (3a).** EIMS (*m/z*, relative intensity) 267/269/271 (M<sup>+</sup>, 24/46/23), 249/251/253 (M–H<sub>2</sub>O, 51/100/50). (–)-ESIMS *m/z* 266/268/270 (M–H<sup>+</sup>, 1/2/1). <sup>1</sup>H NMR (300 MHz, MeOD)  $\delta$  6.82 (s, H-3). <sup>13</sup>C NMR (75 MHz, MeOD)  $\delta$  126.3 (s, C-2), 118.5 (d, C-3), 100.4 (s, C-4), 107.4 (s, C-5), 162.6 (s, C-6).

**5.3.4. 4,5-Dibromopyrrole-2-carboxylic acid TFA adduct (3b).** EIMS (*m/z*, relative intensity) 267/269/271 (M<sup>+</sup>, 24/46/23), 249/251/253 (M–H<sub>2</sub>O, 51/100/50). (–)-ESIMS *m/z* 266/268/270 (M–H<sup>+</sup>, 1/2/1). <sup>1</sup>H NMR (300 MHz, MeOD)  $\delta$  6.90 (s, H-3). <sup>13</sup>C NMR (75 MHz, MeOD)  $\delta$  125.9 (s, C-2), 118.4 (d, C-3), 100.4 (s, C-4), 107.6 (s, C-5), 162.5 (s, C-6).

**5.3.5. Oroidin base (4a).** EIMS (*m/z*, relative intensity) 266/268/270 (M-121<sup>+</sup>, 11/22/11), 249/251/253 (M-121-NH<sub>3</sub><sup>+</sup>, 15/30/15). (+)-ESIMS *m/z* 388/390/392 (M+H<sup>+</sup>, 1/2/1). <sup>1</sup>H NMR (600 MHz, MeOD) and <sup>13</sup>C NMR (75 MHz, MeOD), see Table 1.

**5.3.6. Oroidin TFA salt (4b).** EIMS (70 eV, *m/z*, relative intensity) 266/268/270 (M-121<sup>+</sup>, 11/22/11), 249/251/253

(M-121-NH<sub>3</sub><sup>+</sup> 15/30/15). (+)-ESIMS *m/z* 388/390/392 (M+H<sup>+</sup>, 1/2/1). <sup>1</sup>H NMR (600 MHz, MeOD) and <sup>13</sup>C NMR (150 MHz, MeOD), see Table 1.

**5.3.7. 3-Amino-1-(2-aminoimidazolyl)-prop-1-ene (5).** (+)-ESIMS *m/z* 139 (M+H<sup>+</sup>), 122 (M-NH<sub>3</sub>+H<sup>+</sup>). <sup>1</sup>H NMR (D<sub>2</sub>O, 300 MHz) δ 3.70 (d, *J* = 6.9 Hz, H<sub>2</sub>-1), 5.98 (dt, *J* = 6.9, 15.4 Hz, H-2), 6.52 (d, *J* = 15.4 Hz, H-3), 6.79 (s, H-5). <sup>13</sup>C NMR (D<sub>2</sub>O, 75 MHz) δ 40.8 (t, C-1), 119.8 (d, C-2), 121.3 (d, C-3), 134.1 (s, C-4), 112.4 (d, C-5), 147.3 (s, C-6).

**5.3.8. Taurine (6).** (–)-ESIMS *m/z* 124 (M–H<sup>+</sup>), 249 (2M–H<sup>+</sup>). <sup>1</sup>H NMR (600 MHz, D<sub>2</sub>O) δ 3.28 (t, *J* = 6.7 Hz), 3.45 (t, *J* = 6.7 Hz). <sup>1</sup>H NMR (600 MHz, DMSO-*d*<sub>6</sub>) δ 2.69 (t, *J* = 6.5 Hz), 3.02 (t, *J* = 6.5 Hz), 7.60 (br s). <sup>13</sup>C NMR (125 MHz, D<sub>2</sub>O) δ 47.4 (t), 35.3 (t). <sup>13</sup>C NMR (125 MHz, DMSO-*d*<sub>6</sub>) δ 47.6 (t), 36.1 (t).

#### 5.4. Preparation of fatty acid methyl esters and GC–MS analyses

For lipid analysis between 0.5 and 2 mg of FAs was dissolved in 5–10 ml of 1.5 M HCl–MeOH and refluxed for 6 h. The reaction mixture was then evaporated to dryness under vacuum. The FA methyl esters thus obtained (1–3 mg) were then purified by silica gel CC using a Pasteur pipette and eluting with hexane/ether (8:2 v/v). The solvent was evaporated to dryness and the methyl esters were then dissolved in hexane and analyzed by GC–MS. The relative GC retention times and mass spectra of the methyl esters, the mass spectra of the corresponding pyrrolidide derivatives, catalytic hydrogenation and dimethyl disulfide derivatization provided the basis for the characterization of the fatty acids.<sup>51</sup> Fatty acid methyl esters, pyrrolidides and dimethyl disulfide derivatives were analyzed by direct ionization using GC–MS (Hewlett–Packard 5972A) at 70 eV equipped with a 30 m × 0.25 mm special performance capillary column (HP-5MS) of polymethylsiloxane cross-linked with a 5% phenyl methylpolysiloxane and He as the carrier gas. The temperature programme was as follows: 130 °C for 1 min, increased at a rate of 3 °C/min to 270 °C and maintained for 30 min at 270 °C.

#### 5.5. In vitro assay for *Plasmodium falciparum*

Antiplasmodial activity was determined using the K1 strain of *P. falciparum* (resistant to chloroquine and pyrimethamine). A modification of the [<sup>3</sup>H]-hypoxanthine incorporation assay was used.<sup>52</sup> Briefly, infected human red blood cells in RPMI 1640 medium with 5% Albumax were exposed to serial drug dilutions in microtitre plates. After 48 h of incubation at 37 °C in a reduced oxygen atmosphere, 0.5 μCi [<sup>3</sup>H]-hypoxanthine was added to each well. Cultures were incubated for a further 24 h before they were harvested onto glass-fibre filters and washed with distilled water. The radioactivity was counted using a Betaplate™ liquid scintillation counter (Wallac, Zurich, Switzerland). The results were recorded as counts per minute (cpm) per well at each drug concentration and expressed as a percentage of the untreated controls. From the sigmoidal inhibition

curves IC<sub>50</sub> values were calculated. Artemisinin was used as reference (Table 2).

#### 5.6. In vitro assays for *Trypanosoma brucei rhodesiense*, *T. cruzi*, *Leishmania donovani* and L6 cell cytotoxicity

Antiparasitic assays for *T. brucei rhodesiense*, *T. cruzi* and the cytotoxicity assay against rat skeletal myoblasts (L6 cells) were performed as described previously.<sup>53</sup> The assay for *L. donovani* was done using the Alamar Blue assay as described for *T. brucei rhodesiense*. Briefly, axenic amastigotes were grown in SM medium<sup>54</sup> at pH 5.4 supplemented with 10% foetal bovine serum. 100 μl of the culture medium with 10<sup>5</sup> amastigotes from axenic culture with or without a serial drug dilution was seeded in 96-well microtitre plates. After 72 h of incubation 10 μl of Alamar Blue was then added to each well and the plates incubated for another 2 h. Then the plates were read with a microplate fluorometer as previously described.<sup>53</sup> Benznidazole, melarsoprol, miltefosine, and podophyllotoxin were used as reference (Table 2).

#### 5.7. *PfFabI* inhibition assay and kinetic studies with oroidin base (4a)

The *PfFabI* assay was carried out as reported.<sup>11,12</sup> Briefly, the extracts or isolated compounds were dissolved in DMSO and tested at 10–100 μg/ml in the presence of 1 μg (22 nM) enzyme and 200 μM NADH in 1 ml of 20 mM Hepes, pH 7.4, and 150 mM NaCl. The reaction was started by addition of 50 μM crotonoyl-CoA (substrate). The enoyl-reductase activity of *PfFabI* was assayed by monitoring the oxidation of NADH to NAD<sup>+</sup> at 340 nm for 1 min. The initial velocities were determined and IC<sub>50</sub> values were estimated from graphically plotted dose–response curves. Triclosan was used as positive control (IC<sub>50</sub> 50 nM = 14 ng/ml).

The inhibition mechanism for **4a** was determined with respect to the substrate crotonoyl-CoA and the cofactor NADH under Michaelis–Menten steady-state conditions. With respect to the substrate, *PfFabI* was incubated with a fixed and saturating NADH concentration (200 μM) and increasing inhibitor concentrations (0–2 μM). The reaction was initiated by the addition of crotonoyl-CoA (10–50 μM). The inhibition mechanism with respect to the NADH was determined in a similar way. To this end, *FabI* was incubated with varying NADH concentrations (10–50 μM) and different inhibitor concentrations (0–2 μM). The reaction was initiated by the addition of 500 μM crotonoyl-CoA. *K<sub>i</sub>* values were obtained from Dixon and secondary plots. The reported values represent means of three independent experiments.

#### 5.8. *MtFabI* and *EcFabI* inhibition assays

Enzyme inhibition assays were performed as described.<sup>47,55,56</sup> *MtFabI* (50 nM) and *EcFabI* (10 nM) were assayed in 30 mM PIPES and 150 mM NaCl buffer at pH 6.8 or pH 8.0, respectively, using 25 μM 2-dodece-

noyl-CoA and 250  $\mu$ M NADH. Enzyme activity was monitored by following the oxidation of NADH at 340 nm. The initial velocities were determined in triplicate at increasing inhibitor concentrations [I], and  $IC_{50}$  values were calculated by fitting the data to equation  $y = 100/(1 + [I]/IC_{50})$  using Grafit 4.0.

### Acknowledgments

D.T. thanks the Dr. Helmut Legerlotz Foundation (University of Zurich), for the fellowship provided in the very early phase of this project. The Turkish Ministry of Agriculture and Forestry is sincerely acknowledged for the permission for sample collection and the assistance at transport. R.O.'N. thanks the NIH-RISE program for a graduate fellowship. This work was partially supported by NIH Grants AI044639 and AI070383 (P.J.T.) and S06GM08102 (N.M.C.).

### Supplementary data

The X-ray crystal structure and crystallographic data of taurine (**6**) are available. Supplementary data associated with this article can be found, in the online version, at doi:10.1016/j.bmc.2007.07.032.

### References and notes

- Smith, S. *FASEB J.* **1994**, *8*, 1248–1259.
- Schweizer, E.; Hoffman, J. *Microbiol. Mol. Biol. Rev.* **2004**, *68*, 501–517.
- Waller, R. F.; Keeling, P. J.; Donald, R. G.; Striepen, B.; Handman, E.; Lang-Unnasch, N.; Cowman, A. F.; Besra, G. S.; Roos, D. S.; McFadden, G. I. *Proc. Natl. Acad. Sci. USA* **1998**, *95*, 12352–12357.
- Banerjee, A.; Dubnau, E.; Quémard, A.; Balasubramanian, V.; Sun Um, K.; Wilson, T.; Collins, D.; de Lisle, G.; Jacobs, W. R., Jr. *Science* **1994**, *263*, 227–230.
- Heath, R. J.; Yu, Y. T.; Shapiro, M. A.; Olson, E.; Rock, C. O. *J. Biol. Chem.* **1998**, *273*, 30316–30320.
- Heath, R. J.; Rubin, J. R.; Holland, D. R.; Zhang, E.; Snow, M. E.; Rock, C. O. *J. Biol. Chem.* **1999**, *274*, 11110–11114.
- Heath, R. J.; Li, J.; Roland, G. E.; Rock, C. O. *J. Biol. Chem.* **2000**, *275*, 4654–4659.
- Surolia, N.; Surolia, A. *Nat. Med.* **2001**, *7*, 167–173.
- Argyrou, A.; Jin, L.; Siconilfi-Baez, L.; Angeletti, R. H.; Blanchard, J. S. *Biochemistry* **2006**, *45*, 13947–13953.
- Argyrou, A.; Vetting, M. W.; Aladegbami, B.; Blanchard, J. S. *Nat. Struct. Mol. Biol.* **2006**, *13*, 408–413.
- Kırmızıbekmez, H.; Çalis, I.; Perozzo, R.; Brun, R.; Dönmez, A. A.; Linden, A.; Rüedi, P.; Tasdemir, D. *Planta Med.* **2004**, *70*, 711–717.
- Tasdemir, D.; Güner, N. D.; Perozzo, R.; Brun, R.; Dönmez, A. A.; Çalis, I.; Rüedi, P. *Phytochemistry* **2005**, *66*, 355–362.
- Itoh, T.; Yoshida, K.; Tamura, T.; Matsumoto, T. *Phytochemistry* **1982**, *21*, 727–730.
- Santalova, E. A.; Makarieva, T. N.; Gorshkova, I. A.; Dmitrenok, A. S.; Krasokhin, V. B.; Stonik, V. A. *Biochem. Syst. Ecol.* **2004**, *32*, 153–167.
- Wright, J. L. C. *Phytochemistry* **1981**, *20*, 2403–2405.
- König, G. M.; Wright, A. D.; Linden, A. *Planta Med.* **1998**, *64*, 443–447.
- Lindel, T.; Hochgürtel, M. *J. Org. Chem.* **2000**, *65*, 2806–2809.
- Hammami, S.; Ben Jannet, H.; Ciavatta, M. L.; Mollo, E.; Cimino, G.; Mighri, Z. *J. Soc. Alger. Chim.* **2006**, *16*, 79–89.
- Wright, A. E.; Chiles, S. A.; Cross, S. S. *J. Nat. Prod.* **1991**, *54*, 1684–1686.
- Briant, C. E.; Jones, D. W. *J. Chem. Cryst.* **1997**, *27*, 481–483.
- Görbitz, C. H.; Prydz, K.; Ugland, S. *Acta Crystallogr., Sect. C* **2000**, *C56*, e23–e24.
- Hibbs, D. E.; Austin-Woods, C. J.; Platts, J. A.; Overgaard, J.; Turner, P. *Chem. Eur. J.* **2003**, *9*, 1075–1084.
- Okaya, Y. *Acta Crystallogr.* **1966**, *21*, 726–735.
- Al-Mourabit, A.; Potier, P. *Eur. J. Org. Chem.* **2001**, 237–243.
- Hoffman, H.; Lindel, T. *Synthesis* **2003**, *12*, 1753–1783.
- Dransfield, P. J.; Dilley, A. S.; Wang, S.; Romo, D. *Tetrahedron* **2006**, *62*, 5223–5247.
- Andrade, P.; Willoughby, R.; Pomponi, S.; Kerr, R. G. *Tetrahedron Lett.* **1999**, *40*, 4775–4778.
- di Giacomo, G.; Dini, A.; Falco, B.; Marino, A.; Sica, D. *Comp. Biochem. Physiol.* **1981**, *74B*, 499–501.
- Dembitsky, V. M.; Rezanka, T.; Srebnik, M. *Chem. Phys. Lipids* **2003**, *123*, 117–155.
- van den Brink, D. M.; Wanders, R. J. *Cell. Mol. Life Sci.* **2006**, *63*, 1752–1765.
- Walther, M. *Comp. Biochem. Physiol.* **2002**, *A133*, 179–190.
- Wang, W.; Lee, Y. M.; Hong, J.; Lee, C.-O.; Park, J. H.; Jung, J. H. *Nat. Prod. Sci.* **2003**, *9*, 241–244.
- Emura, C.; Higuchi, R.; Miyamoto, T. *Tetrahedron* **2006**, *62*, 5682–5685.
- Kawakami, A.; Miyamoto, T.; Higuchi, R.; Uchiumi, T.; Kuwano, M.; Van Soest, R. W. M. *Tetrahedron Lett.* **2001**, *42*, 3335–3337.
- Ishiyama, H.; Ishibashi, M.; Ogawa, A.; Yoshida, S.; Kobayashi, J. *J. Org. Chem.* **1997**, *62*, 3831–3836.
- Kobayashi, J.; Inaba, K.; Tsuda, M. *Tetrahedron* **1997**, *53*, 16679–16682.
- Utkina, N. K.; Fedoreev, S. A.; Maksimov, O. B. *Khim. Prir. Soedin.* **1984**, *4*, 535–536.
- Fattorusso, E.; Tagliatalata-Scafati, O. *Tetrahedron Lett.* **2000**, *41*, 9917–9922.
- Jimenez, C.; Crews, P. *Tetrahedron Lett.* **1994**, *35*, 1375–1378.
- Perozzo, R.; Kuo, M.; Sidhu, A. S.; Valiyaveetil, J. T.; Bittman, R.; Jacobs, W. R. D., Jr.; Fidock, A.; Sacchetti, J. C. *J. Biol. Chem.* **2002**, *277*, 13106–13114.
- Pidugu, L. S.; Kapoor, M.; Surolia, N.; Surolia, A.; Suguna, K. *J. Mol. Biol.* **2004**, *343*, 147–155.
- Ferrari, V.; Cutler, D. J. *Biochem. Pharmacol.* **1991**, *42*, 69–79.
- Yayon, A.; Cabantchik, Z. I.; Ginsburg, H. *Proc. Natl. Acad. Sci. USA* **1985**, *82*, 2784–2788.
- Lindel, T.; Hoffman, H.; Hochgürtel, M.; Pawlik, J. R. *J. Chem. Ecol.* **2000**, *26*, 1477–1496.
- Mohammed, R.; Peng, J.; Kelly, M.; Hamann, M. T. *J. Nat. Prod.* **2006**, *69*, 1739–1744.
- Kelly, S. R.; Jensen, P. R.; Henkel, T. P.; Fenical, W.; Pawlik, J. R. *Aquat. Microb. Ecol.* **2003**, *31*, 175–182.
- Sullivan, T. J.; Truglio, J. J.; Boyne, M. E.; Novichenok, P.; Zhang, X.; Stratton, C. F.; Li, H.-J.; Kaur, T.; Amin, A.; Johnson, F.; Slayden, R. A.; Kisker, C.; Tonge, P. J. *ACS Chem. Biol.* **2006**, *1*, 43–53.
- McFadden, G. I.; Reith, M.; Munholland, J.; Lang-Unnasch, N. *Nature* **1996**, *381*, 482.

49. Zheng, C. J.; Yoo, J. S.; Lee, T. G.; Cho, H. Y.; Kim, Y. H.; Kim, W. G. *FEBS Lett.* **2005**, *579*, 5157–5162.
50. Krugliak, M.; Deharo, E.; Shalmiev, G.; Sauvain, M.; Moretti, C.; Ginsburg, H. *Exp. Parasitol.* **1995**, *81*, 97–104.
51. Carballeira, N. M.; Montano, N.; Vicente, J.; Rodríguez, A. D. *Lipids* **2007**, *42*, 519–524.
52. Matile, H.; Pink, J. R. L. In *Immunological Methods*; Lefkovits, I., Pernis, B., Eds.; Academic Press: San Diego, 1990; pp 221–234.
53. Sperandio, N. R.; Brun, R. *ChemBioChem* **2003**, *4*, 69–72.
54. Cunningham, I. J. *Protozool.* **1977**, *24*, 325–329.
55. Parikh, S. L.; Xiao, G.; Tonge, P. J. *Biochemistry* **2000**, *39*, 7645–7650.
56. Rafi, S.; Novichenok, P.; Kolappan, S.; Zhang, X.; Stratton, C. F.; Rawat, R.; Kisker, C.; Simmerling, C.; Tonge, P. J. *J. Biol. Chem.* **2006**, *281*, 39285–39293.